Synthesis of Tin-Oxide One-Dimensional Nanomaterials and Their Characteristics

Hyoun Woo KIM* and Seung Hyun SHIM

School of Materials Science and Engineering, Inha University, Incheon 402-751

We synthesized one-dimensional (1D) nanomaterials of tin oxide (SnO_2) by carrying out the thermal evaporation of solid Sn powders and varying the O_2 partial pressure in an Ar/O_2 ambient gas. We analyzed the samples with scanning electron microscopy, X-ray diffraction, transmission electron microscopy and photoluminescence (PL). Reactions with a higher O_2 content mainly gave rise to wider or thicker structures. The obtained 1D nanomaterials were single crystalline with a tetragonal rutile structure. The PL spectrum exhibited visible light emission.

I. INTRODUCTION

Tin oxide (SnO_2), an n-type semiconductor with a wide band gap ($E_g = 3.6$ eV at 300 K), is regarded as one of the most promising materials for gas sensors, heat mirrors, photovoltaic solar energy conversion devices, and transparent electrodes because of its good conductivity and transparency in the visible region of the spectrum [1–3]. Inorganic materials with different morphologies and sizes can exhibit different properties [4] even if they are made up of the same elements. Due to their unique properties and promising applications in electrical, optical, and magnetic devices [5–8], one-dimensional (1D) structures have attracted a great deal of attention. Accordingly, apart from the well-studied SnO_2 thin films [9–11], various structural and morphological forms of 1D SnO_2 materials have been fabricated over the past several years, including wire-like structures with circular cross-section [12–15] and ribbon- or belt-like structures with rectangular cross-sections [16–21].

The 1D nanostructure, due to its special morphology, may be an ideal system for fully understanding dimensionally confined transport phenomena and for fabricating functional nanodevices. For further investigations of the novel physical properties and preferred designs of nanodevices, 1D nanostructures with various sizes and shapes need to be fabricated by controlled growth. However, to present, there have been few reports on the effects of processing conditions on the growth or the characteristics of the products. In the present research, we have demonstrated the synthesis of SnO_2 1D nanomaterials by employing a simple evaporation of Sn powders

at various partial pressures of the O_2 ambient gas. We investigated the samples with respect to their structural and photoluminescence (PL) characteristics.

II. EXPERIMENTS

The synthesis process was carried out in a quartz tube (diameter: 55 mm). The source material was pure Sn powders. We employed Au-coated Si substrates. In order to fabricate the Au-coated Si substrates, we used Si as the starting material onto which a layer of Au (about 150 nm) was deposited by using radio-frequency magnetron sputtering. On top of the alumina boat with the source material, a piece of the substrate was placed with the Au-coated side downwards. The vertical distance between the boat and the substrate, which were in the middle of quartz tube, was approximately 10 mm. The quartz tube was inserted into a horizontal tube furnace. During the experiment, the furnace was maintained at a temperature of 900 °C with the ambient gas (Ar + O_2) being at a constant total pressure of 1 Torr. Since our objective was to investigate the effect of O_2 gas injection, the percentages of the O_2 and the Ar partial pressures, respectively, were set to 3 and 97 %, 4 and 96 %, and 6 and 94 %. After the system had been cooled down to room temperature after 2 h of typical deposition, white wool-like products were found on the substrate surface.

The as-grown samples were characterized and analyzed by using glancing-angle X-ray diffraction (XRD, Philips X'pert MRD) with an incidence angle of 0.5°, scanning electron microscopy (SEM, Hitachi S-4200), and transmission electron microscopy (TEM, Philips CM-200). For the TEM observation, the products were

*E-mail: hwkim@inha.ac.kr; Fax: +82-32-862-5546

ultrasonically dispersed in acetone, and a drop of the solution was placed on a Cu grid coated with a porous carbon film. PL measurements were performed by using a He-Cd laser line (325 nm, 55 mW) as the excitation source at room temperature.

III. RESULTS AND DISCUSSION

Figure 1 shows the XRD patterns recorded from the samples using different partial pressures of O_2 gas. The Miller indices are indicated on each diffraction peak. All sharp peaks can be clearly indexed to the tetragonal rutile structure of SnO_2 with lattice constants of $a = 4.738$ Å and $c = 3.187$ Å (JCPDS File No. 41 − 1445). No reflection peaks from the impurities, such as unreacted Sn or other tin oxides, were observed, indicating the high purity of the products. In the XRD measurements, the angle of the incident beam to the substrate surface was approximately 0.5°, and the detector was rotated to scan the samples. Therefore, we surmise that the peaks are mainly from the products. These results indicate that products are pure SnO_2 phase, regardless of O_2 partial pressure in the range of 3 − 6 %.

Figures 2(a), 2(b), and 2(c) show typical top-view SEM images of the samples for O_2 partial pressures of 3, 4, and 6 %, respectively, revealing that the products mainly consist of 1D materials, regardless of the O_2 partial pressure during the synthetic process. Statistical analysis of many SEM images indicated that the width
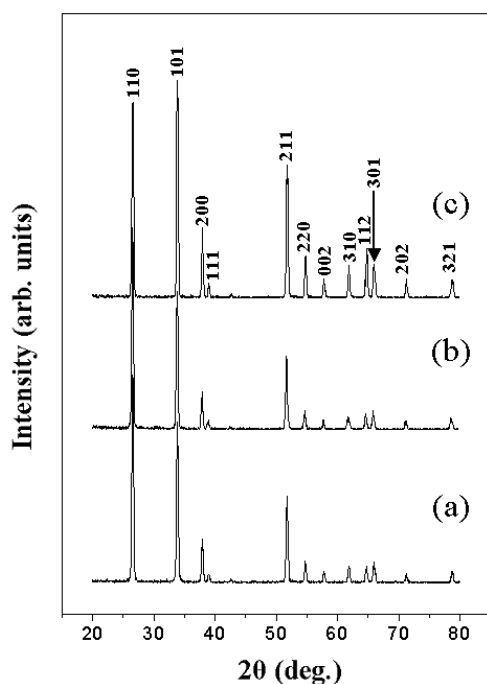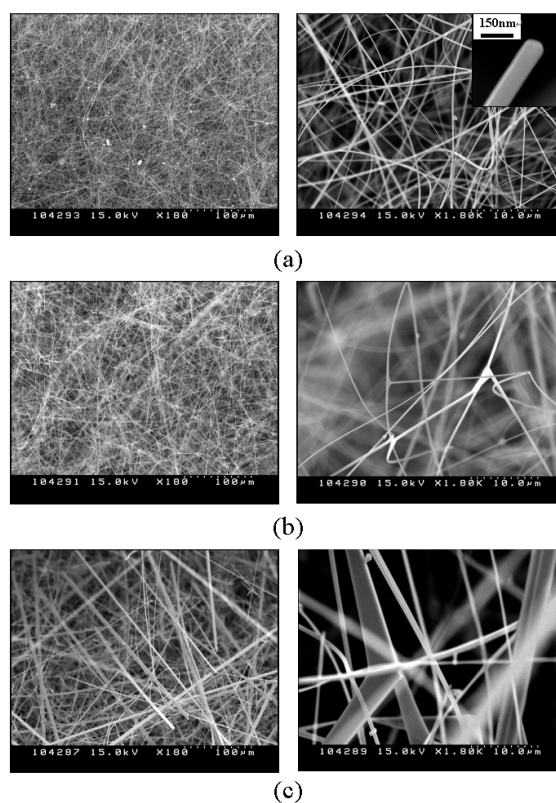

(a)

(b)

(c)

Fig. 2. SEM images of the products for various O_2 partial pressures: (a) 3 %, (b) 4 %, and (c) 6 %. The Inset in Figure 2(a) is a closer view showing the tip of a 1D nanomaterial.

Fig. 1. XRD patterns of the products for various O_2 partial pressures: (a) 3 %, (b) 4 %, and (c) 6 %.

(in case of a rectangular cross-section) or diameter (in case of a circular cross-section) of the SnO_2 1D nanomaterials produced with O_2 partial pressures of 3, 4, and 6 %, respectively, were in the range of 50 − 500 nm, 150 nm − 1.8 μm, and 400 nm − 6.3 μm. These results indicate that the average width or diameter of the structures increases overall with increasing O_2 partial pressure in the range of 3 − 6 %. The upper right inset in Figure 2(a) reveals that no catalyst particle can be seen at the tips of the 1D structures.

TEM analysis of individual 1D nanomaterial provides further insight into the structural properties. A magnification TEM image is shown in Figure 3(a), indicating that the individual structure has a straight and almost uniform width or diameter along its length. The 1D structures are also observed to be almost electron transparent, which further suggests that the structures shown in Figure 3(a) are belt-like with relatively small thicknesses compared to their widths. In the TEM image in the bottom right inset of Figure 3(a), no metal particle can be seen at the ends of the structure, which agrees with the SEM image. The associated selected area electron diffraction (SAED) pattern (Figure 3(b)), recorded perpendicular to the long axis, can be indexed for the $[0\bar{1}1]$ zone axis of a tetragonal rutile SnO_2. The SAED pattern indicates that the SnO_2 structure is single crys-
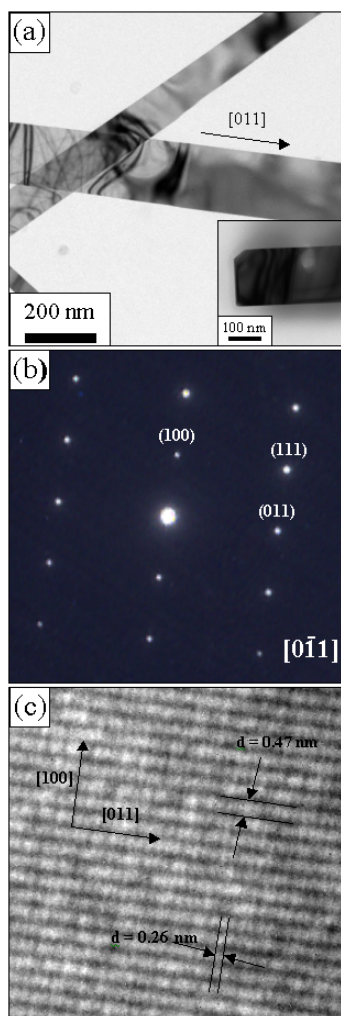
Fig. 3. (a) Low magnification TEM image of SnO_2 1D nanomaterials. The inset shows the end of a nanomaterial. (b) Corresponding SAED pattern of the $[0\bar{1}1]$ zone axis and (c) HRTEM image.

Fig. 4. Room-temperature PL spectrum with an excitation wavelength at 325 nm.

talline and grew along the [011] direction. A representative high resolution TEM (HRTEM) image enlarging part of the structure in Figure 3(a) is given in Figure 3(c). The interplanar spacings are about 0.47 nm and 0.26 nm, corresponding, respectively to the (100) and the (011) planes of tetragonal rutile SnO_2.

In the present work, although Au-coated substrates were employed, from the SEM and the TEM analyses, there is no evidence that a catalyst is present at tips of the structures. Therefore, the growth of the SnO_2 structure in the present route cannot be dominated by a vapor-liquid-solid mechanism. This type of growth, which is close to a vapor-solid process, might be attributed to a diffusion-limited process in a supersaturated environment [22]. The variation of the width or the diameter with the O_2 content indicates that O_2 gas plays an important role in controlling nucleation and growth of SnO_2 1D nanomaterials (Figure 2). The melting points
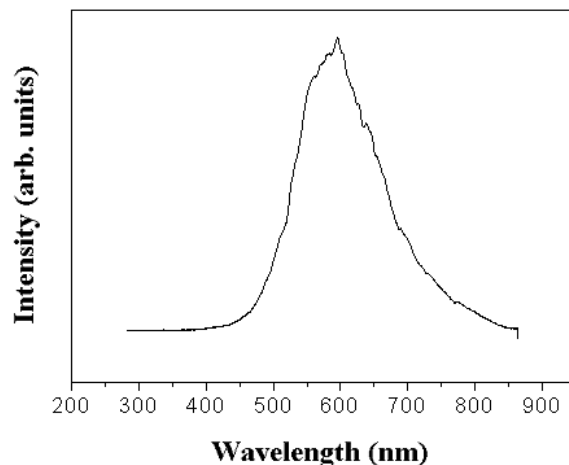
of Sn and SnO_2, respectively, are approximately 232 °C and 1630 °C. At a synthesis temperature of 900 °C in the present study, liquid Sn will oxidize rapidly in the presence of oxygen gas, ultimately resulting in the production of solid SnO_2. It is generally agreed that the SnO forms at the initial stage of oxidation of Sn ($2Sn + O_2 \longrightarrow 2SnO$) and that the SnO is metastable, spontaneously decomposing into liquid Sn and solid SnO_2 according to the reaction: $2SnO \longrightarrow SnO_2 + Sn$ [23–25]. At the processing temperature, the SnO vapor can be transported to the substrate [18]. The higher oxygen partial pressure provides additional oxygen, which may facilitate a large supersaturation of O_2 gas, subsequently leading to a large supersaturation of SnO in its gaseous state and resulting in a fast condensation of solid SnO_2 on the substrate. Therefore, a large supersaturation may acitivate secondary growth sites and heterogeneous nucleation on the side of the 1D structures, tending to produce wider or thicker structures. Under small supersaturation, however, narrow 1D structures are easy to grow. This result is similar to that of a previous work reporting on the growth of Ga_2O_3, in which a small oxygen supersaturation facilitated the growth of 1D nanomaterials [26].

When the synthesis was carried out under the same conditions as those in the present work with an oxygen partial pressure of 3 %, except that SiO_2 substrates were used in the absence of Au layers, we obtained cluster-like structures without any 1D nanomaterial (not shown here). We surmise that the SiO_2 substrate provides additional oxygen at high substrate temperatures [27] and tends to produce the thicker structures instead of thin 1D nanomaterials. We surmise that Au is not easy to oxidize; thus, the elemental Au provides less additional oxygen to the growing SnO_2 nanostructures, contributing to the production of 1D nanomaterials. Efforts are now in progress to pursue these routes in more detail to reveal the synthesis mechanism.

The PLs for the samples obtained with various O_2 par-

tial pressures are almost identical, and a typical room-temperature PL spectrum is shown in Figure 4. The products have a strong peak centered at around 595 nm (corresponding to 2.09 eV). The visible light emission spectrum is similar to that of SnO_2 1D nanomaterials previously synthesized by using laser ablation [28] and solution phase growth [29]. The visible light emission of SnO_2 is known to be related to defect levels within the band gap of SnO_2, associated with O vacancies or Sn interstitials that formed during the synthesis process [28–30].

IV. CONCLUSIONS

In summary, we report the preparation of SnO_2 1D nanomaterials by heating Sn powders under various O_2 partial pressures at 900 °C. The O_2 partial pressure determines the morphology of the final nanostructures. The resulting SnO_2 structures are single crystlalline. No Au-containing nanoparticles are observed on the ends of the as-synthesized SnO_2 1D nanomaterials. We speculate about the mechanism by which the O_2 content affects the morphology. The room-temperature PL spectrum shows an apparent visible light emission band centered at 595 nm.

ACKNOWLEDGMENTS

REFERENCES

[1] Z. M. Jarzebski and J. P. Maraton, J. Electrochem. Soc. **123**, 199 (1976).
[2] V. Vasu and A. Subrahmanyam, Thin Solid Films **193-194**, 973 (1990).
[3] A. Tsunashima, J. Mater. Sci. **21**, 2731 (1986).
[4] J. Hulliger, Chemistry and Crystal Growth, Angew. Chem., Int. Ed. Engl. **33**, 143 (1994).
[5] E. W. Wong, P. E. Sheeham and C. M. Lieber, Science **277**, 1971 (1997).
[6] K. Bubke, H. Gnewuch, M. Hempstead, J. Hammer and M. L. H. Green, Appl. Phys. Lett. **71**, 1906 (1997).
[7] A. Helimann, P. Jutzi, A. Klipp, U. Kreibig, R. Neuendorf, T. Sawitowski and G. Schmid, Adv. Mater. **10**, 398 (1998).
[8] J. Y. Kim, H. W. Shim, E-K. Suh, T. Y. Kim, S. H. Lee, Y. H. Mo and K. S. Nahm, J. Korean Phys. Soc. **44**, 137 (2004).
[9] G. Choi, H. Ryu, Y. Seo, W. Lee, K. Hong, D. Shin, J. Park and S. A. Akbar, J. Korean Phys. Soc. **43**, L967 (2003).
[10] W. Lee, Y. Choi, K. Hong, N-H. Kim, Y. Park and J. Park, J. Korean Phys. Soc. **46**, L756 (2005).
[11] W-P. Tai and J-H. Oh, Thin Solid Films **422**, 220 (2002).
[12] M. Zhang, G. Li, X. Zhang, S. Huang, Y. Lei and L. Zhang, Chem. Mater. **13**, 3859 (2001).
[13] R-Q. Zhang, Y. Lifshitz and S-T. Lee, Adv. Mater. **14**, 1029 (2003).
[14] A. Kolmakov, Y. Zhang, G. Cheng and M. Moskovits, Adv. Mater. **15**, 997 (2003).
[15] J. K. Jian, X. L. Chen, T. Xu, Y. P. Xu, L. Dai and M. He, Appl. Phys. A **75**, 695 (2002).
[16] Z. R. Dai, Z. W. Pan and Z. L. Wang, Solid State Commun. **118**, 351 (2001).
[17] Z. L. Wang and Z. Pan, Adv. Mater. **14**, 1029 (2002).
[18] J. Q. Hu, X. L. Ma, N. G. Shang, Z. Y. Xie, N. B. Wong, C. S. Lee and S. T. Lee, J. Phys. Chem. B **106**, 3823 (2002).
[19] X. S. Peng, L. D. Zhang, G. W. Meng, Y. T. Tian, Y. Lin, B. Y. Geng and S. H. Sun, J. Appl. Phys. **93**, 1760 (2003).
[20] X. L. Ma, Y. Li and Y. L. Zhu, Chem. Phys. Lett. **376**, 794 (2003).
[21] S. H. Sun, G. W. Meng, Y. W. Wang, T. Gao, M. G. Zhang, Y. T. Tian, X. S. Peng and L. D. Zhang, Appl. Phys. A **76**, 287 (2003).
[22] J. Guojian, Z. Hanrui, Z. Jiang, R. Meiling, L. Wenlan, W. Fengying and Z. Baolin, J. Mater. Sci. **35**, 63 (2000).
[23] D-W. Yuan, R-F. Yan and G. Simkovich, J. Mater. Sci. **34**, 2911 (1999).
[24] J. C. Nover and F. D. Richardson, Trans. Inst. Min. Metall. **81**, 63 (1972).
[25] Z. R. Dai, Z. W. Pan and Z. L. Wang, Adv. Funct. Mater. **13**, 9 (2003).
[26] J-S. Lee, K. Park, S. Nahm, S-W. Kim and S. Kim, J. Cryst. Growth **244**, 287 (2002).
[27] B. Y. Geng, L. D. Zhang, G. W. Meng, T. Xie, X. S. Peng and Y. Lin, J. Cryst. Growth **259**, 291 (2003).
[28] J. Hu, Y. Bando, Q. Liu and D. Goldberg, Adv. Func. Mater. **13**, 493 (2003).
[29] B. Cheng, J. M. Russell, W. Shi, L. Zhang and E. T. Samulski, J. Am. Chem. Soc. **126**, 5972 (2004).
[30] S-S. Chang and D. K. Park, Mater. Sci. Eng. B **95**, 55 (2002).